Performance evaluation of aerogel-based and perlite-based prototyped insulations for internal thermal retrofitting: HMT model validation by monitoring at demo scale

R. Galliano [a,*], K. Ghazi Wakili [b], Th. Stahl [c], B. Binder [b], B. Daniotti [a]

[a] *Polimi, Department of Architecture, Built Environment and Construction Engineering, Via Ponzio 31, Milano 20133, Italy*
[b] *Empa, Swiss Federal Laboratories for Materials Science and Technology, Überlandstrasse 129, Dübendorf 8600, Switzerland*
[c] *R&D Fixit Gruppe, Fixit AG, Im Schachen 416, Holderbank 5113, Switzerland*

A South-East oriented faç ade of a protected building of Politecnico di Milano has been retrofitted on its inner surface with respect to energy consumption and thermal comfort. Four prototype solutions including special perlite boards and aerogel composite materials have been used. The analysis envisaged both monitoring by means of temperature, moisture and heat flux sensors at demo scale, and Heat and Moisture Transfer modelling. The study has been carried out before and after retrofit. The present investigation is concerned with the comparison between simulation and measurements. A parametric analysis permitted both the validation of assumptions made for numerical simulations and the identification of the most affecting variables.

Keywords:
Retrofit
Wireless monitoring
Historic building
Hygrothermal performance
Aerogel based material
Perlite based material
Heat and moisture transfer

1. Introduction

According to the Directive 2012/27/EU [1], based on the conclusions lead by the Council on the Energy Efficiency Plan 2011, the construction sector causes 40% of the energy consumption. In Europe, 9 billion square meters of the residential stock have been built before 1975 with high energy demand. Among them one third are multi-owner, multi-storey residential buildings [2]. Often, the only acceptable solution for the energy efficiency improvement of the envelope is the internal retrofitting of the perimeter walls. The type of insulation selected for the retrofitting can affect the results, especially in case of inner retrofit. The use of novel and high performance insulation could be competitive to the conventional one, in terms of equivalent thickness for reaching the same performance. This has been demonstrated also in United States by means of cost-effectiveness analysis [3]. Over the last 5 years several state-of-the-art reviews [4–6] and innovative developments [7] inspected the application of aerogel as thermal insulation in buildings. It stands for a large interest in this novel material, due to the low thermal conductivity and its versatility, especially if used as a composite product. The aerogel-based products have a thermal conductivity in general below 0.025 $W m^{-1} K^{-1}$. Aerogel itself has a very low thermal conductivity around 0.015 $W m^{-1} K^{-1}$ because of high porosity, low gaseous conduction and low radiative conduction. Convective heat transfer is negligible in case of pores smaller than 1 mm. The low gaseous conductivity is explained by the Knudsen effect, which represents the ratio between the mean free path of the gas molecules and the characteristic diameter of the pores. The radiative transfer is dominant at high temperature (above 200 °C). A comprehensive analysis of the synthesis, properties and applications of aerogel based products has been presented recently [8,9].

Because of the critical aspects, especially in case of inner retrofit, the hygrothermal risk assessment becomes a priority [10–12]. This can be done by means of a hygrothermic modelling of the wall to forecast the behaviour by means of calculation. Several parameters can affect the result of numerical simulations. For that reason, a sensitivity analysis should be carried out, to take into account the uncertainties, especially those related to material properties and climatic conditions. As demonstrated by Holm and Kuenzel

* Corresponding author.
E-mail address: rosanna.galliano@polimi.it (R. Galliano).

Published Journal Article available at: http://dx.doi.org/10.1016/j.enbuild.2016.05.021

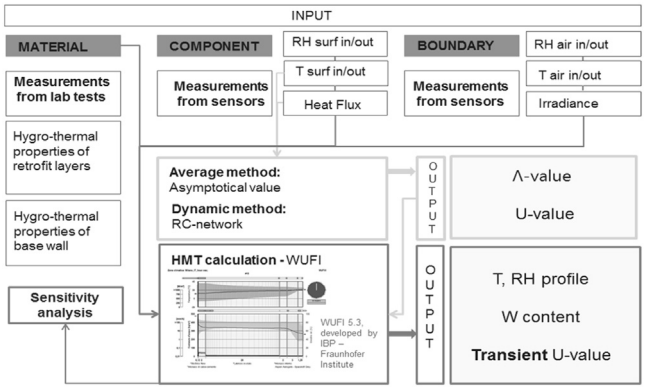

Fig. 1. Detailed scheme of the input, output data and the methods of analysis.

[13] the higher influence is given by weather data, indoor moisture load, liquid transport and moisture retention, whereas the thermal conductivity itself does not affect sensitively the results. This has also been confirmed by Hens [14], where the importance of hygrothermal load is related to the initial moisture content, the latent heat and the wind driven rain, together with the quality of the airtightness. The probabilistic approach, in terms of uncertainty of the parameters effects on the results, has been followed also for the wetting process of a massive wall with interior retrofit [15] and for evaluating the impact factors on the thermal performance of hol-low brick wall [16]. A Monte Carlo analysis presented in Vereecken et al. [17] evaluates the correlation between initial input data and results in terms of energy savings and hygrothermal risks for inter-nal retrofit. Monte Carlo approach has been used also for a proposal of a stochastic material database [18].

For a complete and reliable assessment of the hygrothermal behaviour, the comparison with real application is necessary as also confirmed by Hens [19]. Many researchers carried out sev-eral studies on different kind of insulating materials by means of in-situ measurements, testing at laboratory scale, compared with model and calculation too [20–31]. In general terms, the aim was the evaluation of relative humidity and temperature profiles and heat flux passing through the wall assembly, for determining the improvement of energy performance (U-value), verifying possible critical events or forecasting the effect on indoor conditions.

The aim of this study is the hygrothermic evaluation of novel insulating systems for internal retrofit of perimeter walls including the influence of real weather data during winter and summer periods. The analysis has been carried out by means of two methods in parallel: measurement of hygrothermic parameters by sensors, monitoring a demo wall; and forecasting of the hygrothermic behaviour by heat and moisture transfer simulation (HMT), as shown in Fig. 1. For the present study, different systems have been worked out within the FP7 European Project EASEE[1] [32]. Aerogel-based composites and perlite composites have been compared as well. They have been designed, produced and characterized to investigate advantages and drawbacks of each one. In summary, the issue deals with the following questions: what is the correlation between measurements and HMT simulation? Which are the most influential parameters for optimizing the retrofit systems? Are the whole lab characterization tests fundamental for the performance forecast? Are the actual environmental parameters fundamental as well?

[1] EASEE: Envelope Approach to improve Sustainability and Energy Efficiency in existing multi-storey multi-owner buildings.

2. Case study and experimental set-up

2.1. Base wall description

The chosen test faç ade for the installation of the inner retrofitting systems is a part of building No.14, situated at the university campus “Leonardo-Città Studi” of Politecnico of Milan. It is Architect Giò Ponti’s design of an eight-storey building, built in 1965 and classified as Cultural Heritage. The building is composed of a concrete and steel structure and non-load bearing cavity walls. The external finishing is composed of vitrified ceramic tiles with a distinctive pattern. Since altering the external surface of the building was not allowed, the internal retrofitting appeared to be the best solution, especially using lower thickness of insulation to keep the reduction of the inner volume of the room at a minimum. The portion of the wall intended to be retrofitted was placed at the sec-ond floor, South-East and South-West oriented and belongs to a meeting/teaching room. The room is equipped with a fan coil sys-tem, working during winter and summer. The system is partially centralized and the user can arbitrarily switch it on or off.

The unventilated cavity wall, from outside to inside, is composed of: vitrified grey ceramic tiles (dimensions: 15 × 7.5 × 0.7 cm), cement base render (2.5 cm), first layer of hollow bricks (12 cm thick), an unventilated air cavity (34.5 cm thick at South-East side and 33.0 cm thick at South-West side), second layer of hollow bricks (8 cm thick) and internal cement lime based plaster with a gypsum finishing (1.5 cm) (Fig. 2). The whole thickness of the wall before retrofit is 59.2 cm. The properties of internal and external render are typical values: the external one has $\lambda = 1.2\ W\,m^{-1}\,K^{-1}$, $\mu = 25$; the internal one has $\lambda = 0.8\ W\,m^{-1}\,K^{-1}$, $\mu = 19$. The properties of the finishing vitrified clay tiles have been taken from technical data provided by the producer of analogous tiles for the external refurbishment, with $\lambda = 1.3\ W\,m^{-1}\,K^{-1}$, $\mu = 285$.

In compliance with the EN 1745:2012 [33] about the thermal properties of the masonry products, the thermal conductivity of each layer of hollow bricks (λ_{BRICKS}) has been calculated considering the thermal conductivity of the brick unit (λ_{UNIT}) and the thermal conductivity of the laying mortar (λ_{MOR}) with their own percentage area. λ_{UNIT}, equal to $0.209\ W\,m^{-1}\,K^{-1}$, is the value taken from technical data sheet of 4-holes horizontally perforated clay bricks (size 8 × 12 × 24 cm), holes 59% and density 650 kg m $^{-3}$; λ_{MOR} is equal to $0.85\ W\,m^{-1}\,K^{-1}$ and is the value for a generic laying cement-lime mortar. The brick units for the outside and inside par-titions are of the same type but laid into different directions. As a result the percentage of area for mortar joints is different, leading to a different value between external and internal layer of hollow bricks: $\lambda_{BRICKS,EXT} = 0.29\ W\,m^{-1}\,K^{-1}$, $\lambda_{BRICKS,INT} = 0.27\ W\,m^{-1}\,K^{-1}$.

For the non-ventilated air layer the effective transport parameters have been determined adjusting the heat conductivity and the diffusion resistance, considering also that the model in WUFI can neither simulate convective and radiative heat transfer nor mass transport in air layers. A thermal resistance $R = 0.183\ m^2\,K\,W^{-1}$ has been calculated according to the standard EN ISO 6946:2008 [34], obtaining $\lambda_{AIR,EQ} = 1.91\ W\,m^{-1}\,K^{-1}$ in function of the thickness and very low vapour resistance $\mu = 0.003$ (calculation method referred to in WUFI).

2.2. Materials and systems for retrofit

Three prototyped retrofit kits have been developed for the inner surface. They are: a natural perlite-based board with an hydrophobic layer in the middle, including gluing and reinforcing renders (kit A.1); an expanded recycled glass based flat panel, with multilayer silica aerogel non-woven polyester textile (kit B.1) and a flexible single-layer silica aerogel non-woven textile with a fabric finishing layer (kit B.2). In addition to those above, a loose-fill hydrophobic

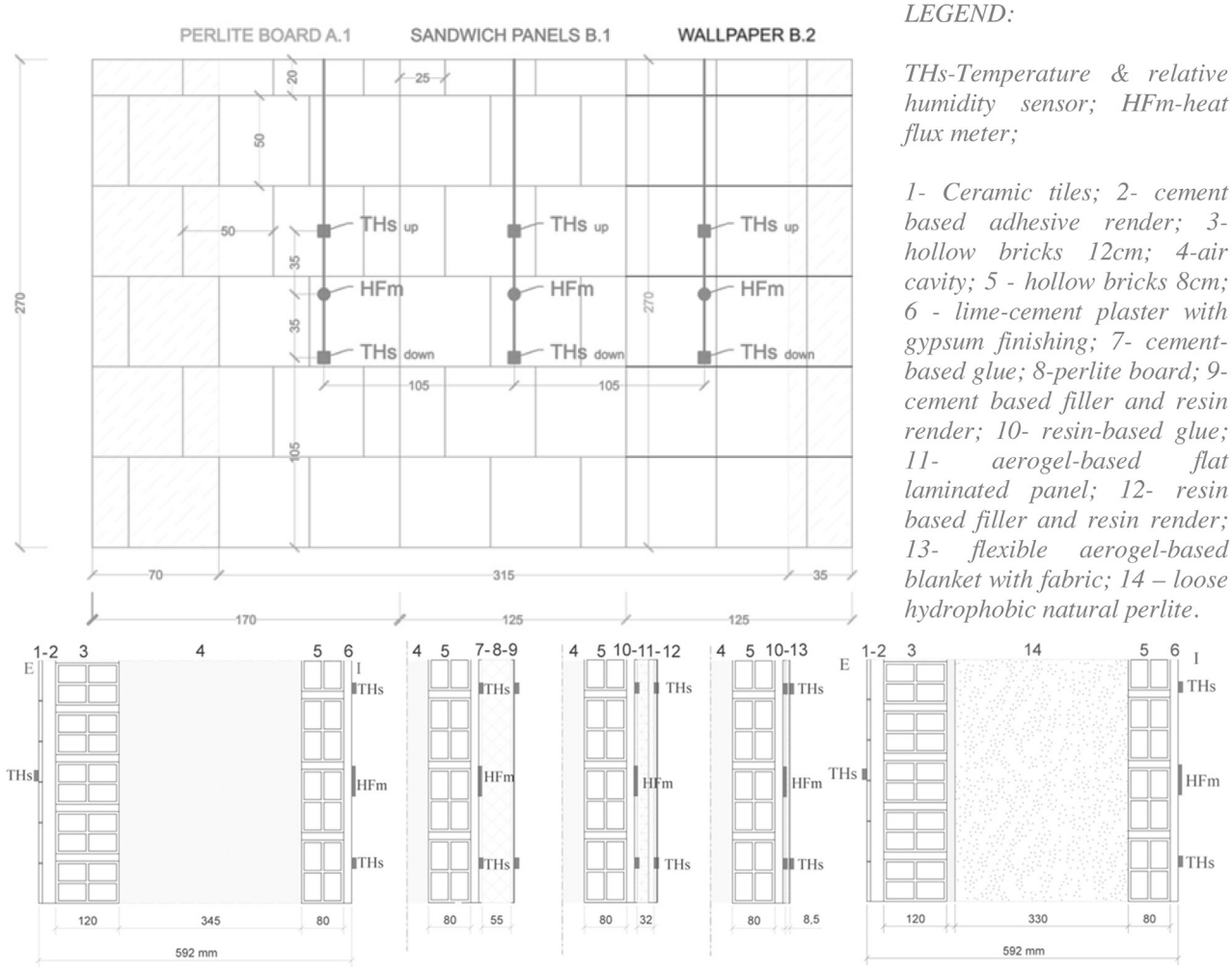

Fig. 2. Vertical cross section and front view of wall partitions and sensor positions.

Table 1
Structure of the retrofit kits.

Type	Adhesive Render	Insulation layer composition	Coating	Finishing coat
A.1	Cement based (4–5 mm)	Board thick 55 mm: hydrophilic natural perlite, mineral binders and additives, with hydrophobic layer in the middle. Weight 12 kg m^{-2}	Cement coating and filler (3–4 mm) with reinforcing glass fibres	Resin based (1.5 mm) with marble powder
B.1	Resin based (4–5 mm)	Three layers of aerogel-PES mat (20 mm), glued to a recycled based board (10 mm) by means of 1.5 mm potassium silicate adhesive. Weight 8.9 kg m^{-2}	Resin coating and filler (3–4 mm) with reinforcing glass fibres	Resin based (1.5 mm) with marble powder
B.2	Resin based (4–5 mm)	Single layer of aerogel-PES mat (7 mm). Weight 1.7 kg m^{-2}	Tri-laminated polyester textile	Tensioned fabric
A.2	–	Loose-fill hydrophobic expanded natural perlite	–	–

natural perlite for cavity wall insulation (kit A.2) has been analysed as a fourth retrofit solution. The retrofit layers are described in Table 1 and Fig. 2.

In case of the perlite board, the hydrophobic layer in the middle of the thickness of panel has been added using a specific procedure under non-disclosure protection. The aim is to limit the absorption of liquid water from external layers of the wall but guarantee water vapour transfer and drying from both directions.

The board is positioned on the wall with a grounding primer on the internal surface for easier application of the render.

The insulating aerogel-PES composite mat is made by allowing sol-gel synthesis among cross-linked fibres using silicon-based compounds as precursors through ageing, and subcritical drying. As result of the process, the air space between the fibres has been filled by aerogel structure [5,35].

For Kit A.2 the loose hydrophobic expanded natural perlite fills the air cavity of 330 mm thickness. Holes were drilled at the top of the wall, allowing the perlite to seep in the cavity simply by gravity.

The materials composing retrofit kits have been tested following the main directives of the reference standards in order to have com-

Table 2
Thermal conductivity of different insulation type and water vapour resistance of the renders.

Insulation	Aerogel-PES		Perlite board		Loose-fill perlite	
λ_{DRY} (W m^{-1} K^{-1})	0.025 ± 0.0005		0.063 ± 0.002		0.046 ± 0.0005	
Render	Cement based		Resin based			Polyester fabric
μ_{DRY} (−)	glue 9.8	filler 6.6	glue/filler 210	coat 190		12

plete data to describe the hygrothermal behaviour. The measured properties are: density by means of volume and weight; thermal conductivity at dry and moist condition (EN 12667-EN 12664); water vapour transmission properties (EN ISO 12572); hygroscopic sorption properties (EN ISO 12571); long-term water absorption by total immersion (EN 12087); water absorption coefficient by partial immersion (EN ISO 15148). All these data have been used as input for the HMT model. Two types of data are shown in Table 2: ther-mal conductivity of the of the insulation layer and water vapour resistance factor of the renders.

The scheme of installation, on the internal side of the South-East part (420 × 270 cm), for the rigid boards and panels, includes modules with different size: kit A.1 (total area of 4.59 m^2) is divided into 15 boards 50 × 50 cm, 8 boards 20 × 50 cm, 1 board 20 × 20 cm; kit B.1 (total area 3.38 m^2) is divided into 10 boards 49 × 49 cm, 5 boards 25 × 49 cm, 2 boards 25 × 49 cm, 1 board 25 × 25 cm; kit B.2 (total area 3.37 m^2) is composed by 2 rolled-up strips 50 × 270 cm, 1 rolled-up strips 20 × 270 cm. The aim was to have the same portion of the cavity wall behind each kit. For that reason, the dimension of each partition takes into account also the existence of columns (distance between them of 315 cm). The South-West side with a total area of 11.61 m^2 has been retrofitted by filling the air cavity with the natural hydrophobic loose perlite (kit A.2), resulting in a volume of 2.93 m^3, subtracting the section of the cavity occupied by the pillars and the pipes.

2.3. Monitoring set-up

A continuous monitoring campaign has been carried out and studied for more than one year, from December 2013 until March 2015. The analysed data include 7 months before retrofit and 8 months after retrofit. Summer and winter periods are available for both conditions. A complete set of sensors, necessary for the thermal conductance evaluation, has been installed for all retrofit solutions.

Humidity and temperature sensors (THs) with a typical accuracy tolerance of ±1.8% RH and ±0.2 °C respectively, have been installed on the external and internal surface of the three wall partitions, before retrofit. On the external side, one sensor for each partition has been applied. On the inner side, two sensors have been installed for each partition at different heights, the first at 105 cm from the floor, the second one at 175 cm. Heat flux meters (HFM) have also been installed on the internal surface of the wall partitions at a height of 135 cm from the floor level (Fig. 2).

Furthermore, inside and outside air temperature and air relative humidity (THa) data are collected. For the outside, a self-aspirating solar radiation shield protects the sensors. It ensures high surface reflectivity and rapid dissipation of heat, preventing the sensors inside from being affected by direct radiation.

A solar pyranometer has measured the irradiance (W m^{-2}) on the South-East facing and on the South-West facing wall. The instrument has a hemispherical view (0–180°), measurement range from 0 to 1750 W m^{-2} and a spectral range of 380–1120 nm.

After the retrofit, additional THs sensors have been installed on the internal side at the same position in height as the previous ones, on the warm side of the insulation layer. Two extra sensors have been installed inside the air cavity at a distance of about 3 cm from the surface of the inner bricks and at about 100 cm distance between them. The aim was to evaluate the trend of temperature and relative humidity and understand how the convective flow inside the gap can affect the values.

Data have been acquired, stored and transferred by means of a wireless communication system and GPRS modem, allowing on-line visualization and downloading data. The recording time step was 6 min and the data were later transformed into hourly values, as average of the 10 values measured during each hour.

The measured values have been used for the calculation of the thermal conductance Λ and of the thermal transmittance U of the façade, before and after retrofit.

The relative humidity measured by the sensors at the differ-ent positions across the wall section was useful for defining the moisture profile during the different periods of the year, consider-ing also the effect of the rain, especially over the measurements at the external surface, where the sensors are installed with an alu-minium tape on the top. On the other hand, the relative humidity measurement was used to verify the time of drying of renders after the application of the retrofits.

In order to have a complete set of climatic data at boundaries, data collected from the weather station (provided by MeteoLab), placed on the roof of the building, have been added. They are the rain measured on the horizontal surface (mm h^{-1}), wind speed (m s^{-1}) after its correction to obtain the value of speed at 50 cm from the horizontal surface, wind direction (0–360°) and long wave radiation (W m^{-2}).

3. U-value calculation

3.1. Theoretical U-value

At steady state, the theoretical Λ_{ST} (W m^{-2} K^{-1}) and U_{ST} (W m^{-2} K^{-1}) have been calculated. The second one is obtained adding to $1/\Lambda$ the standard surface thermal resistances (R_{si} = 0.13 m^2 K W^{-1}, R_{se} = 0.04 m^2 K W^{-1}) from EN ISO 6946 and doing the reciprocal.

3.2. Determination of U-value by average method

The measured surface temperatures and heat flux have been used for estimating Λ_{AM} of the wall before and after retrofit with the progressive "Average Method" according to ISO 9869-1 [36] by means of the equation below:

$$\Lambda_{AM} = \frac{\sum_{j=1}^{n} q_j}{\sum_{J=1}^{n} \left(T_{sij} - T_{sej}\right)}$$

An appropriate time interval with relatively stable conductance values has been selected to avoid periods of the year where the progressive average of T_{si} is crossing the progressive average of T_{se}, resulting in a division by zero.

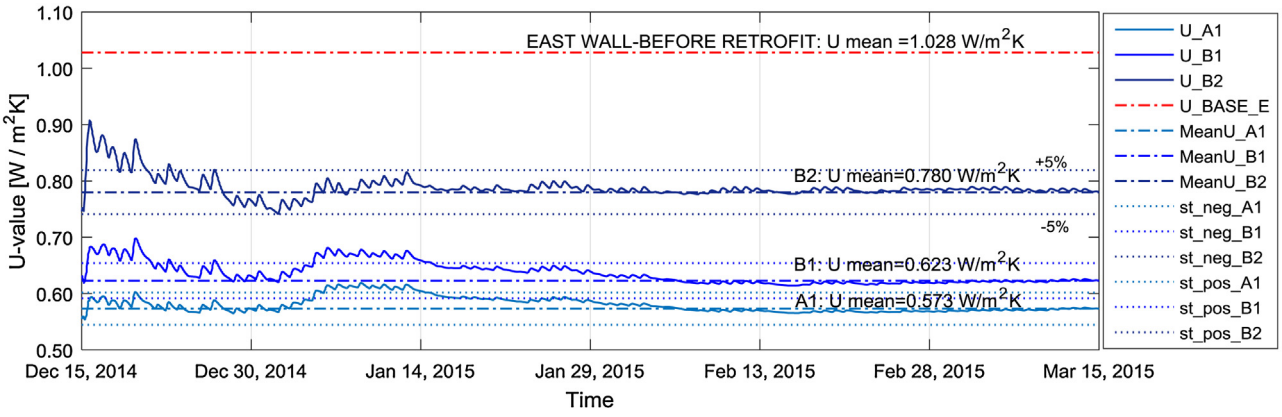

Fig. 3. Thermal transmittance, U-value by average method for cases A.1, B.1 and B.2, with mean value and ±5% range, compared to the base wall.

The Λ-value represents the asymptotical values at the end of three months period, from 15 December to 15 March, corresponding to the wintertime and selected as a stable period. The same period has been considered, a year later, i.e. after retrofit. The progressive average values of heat flux q, inside surface temperature T_{si} and outside surface temperatures T_{se} have been calculated for each partition of the wall. The U-value has been calculated indirectly, using the reference values $R_{si} = 0.13\ m^2\ K\ W^{-1}$, $R_{se} = 0.04\ m^2\ K\ W^{-1}$. The U-value determined by average method for the three inner retrofit kits is in Fig. 3. As the data was collected during more than three months, the acquired measurements are sufficient for obtaining an asymptotical value within the range of ±5%. Because of the high variability of the values measured for retrofit A.2 and the low thermal transmittance, the average method was not applicable. The variability was due to the proximity of heat sources (both fan coil and solar radiation from window).

The accuracy of measurements depends on the accuracy of the calibration of HFM and temperature sensors, the accuracy of data logging system, the random variations caused by differences in the thermal contact between sensors and surface, the operational error of the HFM and errors caused by the variation over time of temperatures and heat flow. In accordance with ISO 9869-1, the theoretical total uncertainty should be between 14% and 28%. In our case, for the evaluation of the total uncertainty, an overall sensor error of ±8% and ±0.5 °C have been assumed for heat flux measurements and inside and outside surface temperature sensors respectively.

3.3. Determination of U-value by the dynamic analysis method

The dynamic analysis method, according to Annex B of the above-mentioned ISO 9869-1, has been applied in order to have results for comparison with the average method. In fact, a South-facing wall is deeply affected by daily fluctuations of the outside surface temperatures, due to solar radiation, and it could be a limitation for the applicability of the average method.

The dynamic analysis has been carried out by means of the software LORD3.2 (Logical R-Determination -Gutschker and Strachan, DYNASTEE), following the so-called RC-networks. The wall is considered as a thermal system and it is modelled as a network of conductances (H) and capacitances (C), with the discretization of the temperature field within the wall itself.

The measured hourly heat flow density and the measured time-dependent surface temperatures represent the boundary conditions, allocated to the border nodes. One of the nodes with measured values is also chosen as output node. A set of linear equations is solved until convergence to determine the unknown parameters (Λ, C. . .). The convergence is verified by comparison between calculated and measured values at the output node. The scheme of nodes for the base wall is represented in Fig. 4. For finding the best fitted value of thermal conductance of the wall, the inner temperature and the heat flux measured at node 6 (N6) are compared, one after the other, with the calculated one. It should be underlined that different parameters affect the in situ measurement. As proven by Cesaratto et al. [24] the random noise of the recorded data does not influence the results significantly. Cesarotto has also demonstrated that dynamic analysis with LORD is suitable for the aim. This method produced reliable results also in case of retrofit A.2, where the average method could not produce accept-able values. In fact, in case of the dynamic method higher variability of the measures does not affect the results and shorter period is enough for the evaluation.

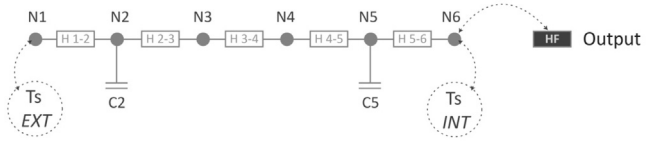

Fig. 4. Scheme of the RC-networks for LORD calculation. Dynamic analysis method.

3.4. Comparison of the results

The results obtained by the different methods are summarized and compared in Table 3. Λ_{ST} is based on calculation with tabulated (or measured, in case of the insulation layers) λ values, but with a reference temperature T = 10 °C and at dry condition RH = 0. Λ_{AM} is the mean asymptotical value with standard deviation, obtained by measurements using the average method. Λ_{DYN} is the mean value with standard deviation obtained by means of dynamic method analysis with LORD.

The difference between Λ_{AM} and Λ_{ST} is up to 16.8% for the base wall, which reveals the underestimation extent of the U-value by the theoretical steady state calculation in dry condition. The difference between Λ_{AM} and Λ_{DYN} is 0.88% for the base wall, and it reaches 4.5% for retrofit A.1, 4.0% for retrofit B1 and 0.1% for B.2. This reveals an agreement between the two methods, with a difference below the 5%, with exception to A.2.

From data collected in Table 3 the improvement of retrofit solutions in thermal conductance has been calculated by the average method and by the dynamic analysis, before and after retrofit and, consecutively, the thermal transmittance of the wall. A decrease in U-value of 44.3% for A.1, 39.4% for B.1 and 24.1% for B.2 is obtained in respect to the base wall. For the solution A.2 the decrease is equal to 89.2%.

Table 3
Conductance and U-value of the wall before and after retrofit. Comparison among methods.

	Λ_{ST}	Λ_{AM}	Λ_{DYN}	U_{ST}	U_{AM}	U_{DYN}
			($W m^{-2} K^{-1}$)			
Base Wall SE	1.069	1.249 ± 0.062	1.260 ± 0.004	0.905	1.028	1.038
Retrofit A.1	0.525	0.641 ± 0.032	0.612 ± 0.002	0.482	0.573	0.554
Retrofit B.1	0.571	0.700 ± 0.035	0.672 ± 0.011	0.521	0.623	0.603
Retrofit B.2	0.829	0.902 ± 0.045	0.903 ± 0.001	0.726	0.780	0.783
Base Wall SW	0.740	0.908 ± 0.045	0.968 ± 0.001	0.657	0.738	0.831
Retrofit A.2	0.126	–	0.091 ± 0.001	0.123	–	0.090

4. Transient heat and moisture transfer model

4.1. Theoretical approach, geometry and properties

The 1-dimensional hygro-thermal behaviour in transient condition of the base wall, and later on the retrofit partitions A.1, B.1, B.2 and A.2 have been assessed, by means of the software Wufi® Pro 5.3, which considers coupled heat and moisture transfer through the assembly [37] and complies with standard EN 15026:2008 [38].

The model of the base wall is composed of one-dimensional layers, from outside to inside, according to the description in the previous section. The material properties of the single layers, composing the base wall, are not directly measured, so they have been selected from the material database, calculated or collected from tabulated design values according to the standards (EN 10456:2007) [39] or obtained from technical data sheet as explained earlier.

The retrofit kits have been modelled on the base of the data described above. In case of kit B.2 in particular, the tri-laminated polyester fabric at the inner side has not been modelled as a layer in the geometry but its s_d-value is considered on the surface, which allows to account for its diffusion-retarding effect. For the Kit A.2 the loose hydrophobic perlite is modelled as a continuous layer with thickness of 33 cm, replacing the air cavity at the South-West side.

The material input data have been derived from the specific laboratory tests, the air cavity has been modelled as explained earlier. The contacts between materials are assumed as ideal and the flows continuous. The assembly has been considered airtight. As outcome, on the one hand the thermal transmittance improvement of the system has been evaluated, on the other hand the most affecting parameters on the results have been highlighted.

4.2. Boundary conditions

Four scenarios have been taken into account. Scenario 1 and 2 are related to the wall before retrofit, scenario 3 and 4 to the wall after retrofit.

"Scenario 1" consists in imposing temperature and moisture gradient on the assembly using the monitored external and internal surface temperature and humidity. Therefore, the boundary conditions are directly imposed on the inner and outer surface, setting the surface heat resistance equal to zero and excluding short-wave and long-wave radiation, as well as rain absorption.

"Scenario 2" consists in setting exterior and interior environment, using the measured data of indoor and outdoor air temperature and air relative humidity, the irradiance measured on the surface and the rain absorption. In that case, surface heat resistances have been considered, as well as solar short-wave radiation absorptivity (α_s) and long-wave radiation emissivity (ϵ) factors of the external surface and vapour diffusion (s_d-value) of the inner surface coating.

"Scenario 3" concerns the after retrofit configuration with boundary conditions directly imposed on the surface as described also in "Scenario 1".

"Scenario 4" uses the measured indoor and outdoor air values as defined also in "Scenario 2", but in that case for the after retrofit configuration (Table 4).

5. Monitoring vs HMT and parametric analysis

5.1. Comparison method

In order to validate the assumption made in the model of wall, by means of parametrical analysis, the comparison between the simulated and the measured values has been carried out. The descriptive statistics have been used to explain the results. The accuracy is verified by correlation, variability and acceptability.

In case of correlation, the coefficient of determination R^2 and linear fit have been used for evaluating the relation between measured (x-axis) and simulated (y-axis) values represented by the scattering of the points. The variability is expressed in terms of maximum, minimum, median and quartiles in the boxplots graph, in which each column represents the difference between simulated and measured value for all combination of parameters. Along this, RMSD value has been calculated and minimized. The acceptability of the results is confirmed by the curves trend over time (hourly values) obtained from simulations using the different parameters combination, compared with the curves obtained by the measure-ments.

5.2. Base wall model validation

Within "Scenario 1", the hourly heat flux resulting from numeri-cal simulation can be compared with the hourly heat flux measured by heat flux meter installed on the wall.

Without the surface heat resistance, the initial thermal conductance Λ-value has been considered equal to 1.256 $W m^{-2} K^{-1}$, according to the results of monitoring.

In order to improve the model fitting into the monitored assem-bly for "Scenario 1" two parameters that can have a larger effect on the results have been modified, leaving the others unchanged: the thermal conductivity of the bricks layers (λ_{BRICKS}) and the initial relative humidity inside the layers, at time zero of simulation ($RH_{t=0}$) (Table 5).

The thermal conductivity of the bricks layer (brick units plus mortar joints) has been considered as influent, considering how much the laying mortar affects the resulting value. The supposed thermal conductivity of the brick leaves, equal to 0.29 $W m^{-1} K^{-1}$ for the external one and 0.27 $W m^{-1} K^{-1}$ for the internal one, are verified considering alternatively the 25% increase and decrease of the thermal conductivity itself.

For the base cavity wall, before retrofitting, the adequate moisture content can be reached at equilibrium by means of parametric analysis using different initial conditions.

As result, the best combination occurs, in general, with no increase or decrease of the design λ-value of the bricks layers and when $RH_{t=0}$ inside the assembly is 78%. It means that the tested wall has higher moisture content with respect to the supposed one at 50%, in general more realistic for an existing wall. One reason

Table 4
Outline of model input data for each scenario.

Input data							
Scenario 1 & 3				Scenario 2 & 4			
Surface boundary condition				Air boundary condition			
Surface transfer coefficients		Climate data/measured in-situ		Surface transfer coefficients		Climate data/measured in-situ	
EXT	INT	EXT	INT	EXT	INT	EXT	INT
				$R_{se} \neq 0$		$T_{A\,EXT}$	$T_{A\,INT}$
$R_{se} = 0$				$s_d = 0$		$RH_{A\,EXT}$	$RH_{A\,INT}$
$s_d = 0$	$R_{si} = 0$	$T_{S\,EXT}$	$T_{S\,INT}$	$\alpha_s \neq 0$	$R_{si} \neq 0$	Irradiance	
$\alpha_s = 0$	$s_d = 0$	$RH_{S\,EXT}$	$RH_{S\,INT}$	$\epsilon \neq 0$	$s_d \neq 0$	Rain	
$\epsilon = 0$				$f_{RAIN} \neq 0$		Wind	
$f_{RAIN} = 0$				SE face			

Table 5
Outline of the validation process, scenario 1 and scenario 2.

Base wall validation process			
Scenario 1		Scenario 2	
(Simulation vs monitoring)		(Simulation vs monitoring)	
HF_{SIM}	HF_{MEAS}	HF_{SIM}	HF_{MEAS}
		$T_{S\,SIM}$	$T_{S\,MEAS}$
		$RH_{S\,SIM}$	$RH_{S\,MEAS}$
Parametric analysis		Parametric analysis	
λ_{BRICKS} ($W\,m^{-1}\,K^{-1}$): initial value – 25% increase – 25% decrease		R_{si} ($m^2\,K\,W^{-1}$): 0.125 – 0.250	
external bricks layer: 0.29 – 0.36 – 0.22		α_s: 0.40 – 0.45 – 0.50 – 0.55 – 0.60	
internal bricks layer: 0.27 –0.34 – 0.20		ϵ: 0 – 0.10 – 0.60 – 0.90	
$RH_{t=0}$: 50% – 65% – 78%		f_{RAIN} (adhering factor): 0 – 0.7 – 1.0	
		R_{se} ($m^2\,K\,W^{-1}$): 0.04 – 0.0588 – Wind-dep – Long-wave rad.	

could be related to the simplification of the air cavity behaviour in the model, where the total heat and water vapour transport are represented by two effective material parameters: thermal conductivity and water vapour resistance, corrected to consider the effect of convention on heat and vapour transport as well.

Within "Scenario 2" it is possible to compare the hourly heat flux, the internal and external surface temperature and relative humidity obtained from simulation and measurements. The parameters, that could be influential, are: solar short-wave absorbance (α_s) and long-wave emissivity (ϵ) of the external tiles, rain absorption and surface heat resistance for inner side (R_{si}) and for outer side (R_{se}) as well (Table 5). All these parameters affect surface temperature and relative humidity.

The solar short wave absorbance and long wave emissivity are affected by the presence of aluminium tape for the protection of the sensors, installed on the outside surface. The final set values are a balance between the characteristics of the tiles and of the aluminium layer at the top. For the solar absorbance coefficient, a range of values between 0.4 and 0.6 has been considered, because of the properties of the tiles (reflectance measured on the tiles is equal to 0.4, absorbance 0.6) and the variation due to the presence of aluminium type (absorbance 0.1). The found optimal value by means of statistical analysis is $\alpha_s = 0.45$.

The external surface heat resistance has been considered as a constant ($0.04\,m^2\,K\,W^{-1}$ from EN ISO 6946 or $0.0588\,m^2\,K\,W^{-1}$ from Wufi predefined value for external wall) or wind-dependant, both with and without the long-wave radiation part (equal to $6.5\,W\,m^2\,K\,W^{-1}$). The best configuration is without wind gains and with no long-wave emission, using $R_{se} = 0.0588\ m^2\,K\,W^{-1}$ (Fig. 5). The reason is that the air temperature and relative humidity, used as input data, are measured at boundary layer next to the surface. If the heat transfer resistance is set as wind-dependent, the changing of surface temperature due to convective flow is considered twice. The same could happen if long-wave radiation emission is used, especially during the night, when the radiative emission of the wall towards clear sky reduces the surface temperature.

The parameter of normal rain, converted into the driving rain load on the surface, has been changed in terms of adhering factor (f_{RAIN}), considering also the condition with no rain absorption. As result the rain load adhering factor, from 0 (no absorption) to 1 (maximum value), does not affect sensitively the results. It is due to the presence of tiles as external layer with water absorption rate less than 0.5% and because of few rainy days along the period of simulation. Even if a moisture source of 1% of driving rain has been added, in the plaster under the tiles (considering for instance a possible crack on the surface or seepage of water between the joints), the results are not considerably changed.

For the inner side, the surface heat resistance R_{si} has been doubled to $0.250\ m^2\,K\,W^{-1}$ with respect to the standard value of $0.125\ m^2\,K\,W^{-1}$ (predefined value in Wufi), achieving best fitting in surface temperature, within $\pm 0.5\ ^\circ C$ range, as demonstrated by the graph (Fig. 6). It means that at the demo wall lower convective flow is acting on the surface. The change takes into account the air convective flow at film surface, which differs at different height of the wall, as demonstrated also in [40–42].

In the case of relative humidity, a satisfactory agreement for the external surface has not been achieved. From the scattering graph, that is clear especially for portion Pre B.1 (before retrofit). When the in-situ sensors measured 100% of relative humidity on the surface (x-axis), due to the moisture storage under the protection of the sensors after a rain event or simply condensation, the model did not reach the same values (y-axis) (Fig. 7).

5.3. Retrofit system model validation

Within "Scenario 3", the hourly heat flux, the temperature and the relative humidity measured at the interface between the base wall and the insulation layer (Fig. 8), and the ones measured inside the air gap, have been compared with the simulated values at the same monitor positions in the model. In this configuration, the effect of material parameters composing the retrofit without influences from the boundaries layers can be understood.

The parametric analysis has been carried out modifying: the thermal conductivity (moisture dependant) of insulating layers, and the water vapour resistance factor (μ), or thickness, of the base and top render. The starting values are the ones measured

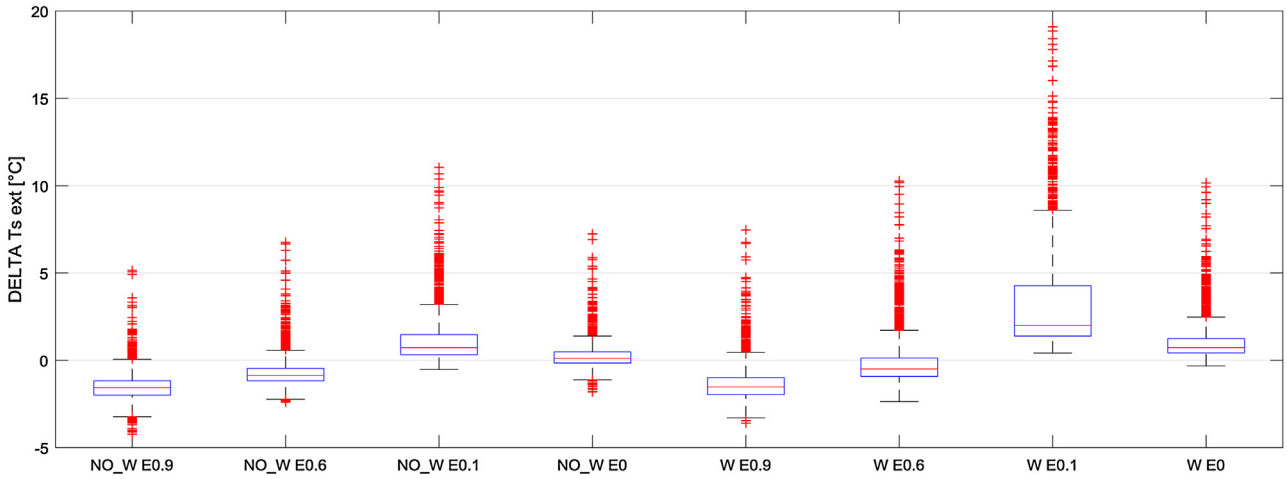

Fig. 5. East wall before retrofit B.1. Scenario 2. Boxplot of the difference between simulated and measured external surface temperature. Each column refers to a different combination of parameters: W, wind-dependent surface heat resistance; NO_W, no wind dependence of surface heat-resistance; E emissivity of the external tiles.

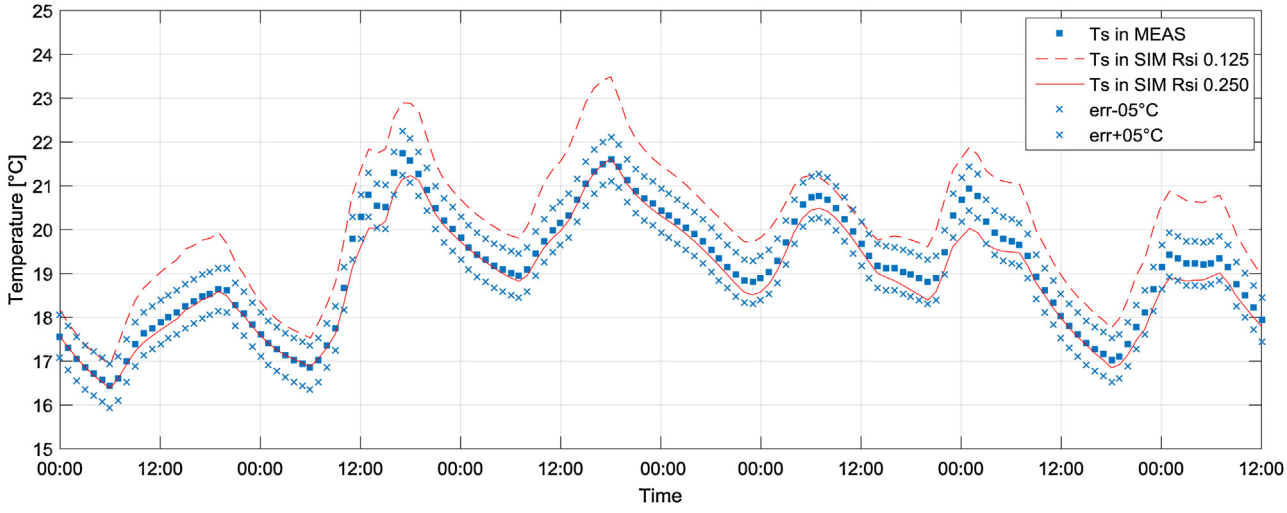

Fig. 6. Curve trend of the inner surface temperature T_{SINT} at wall portion B.1 before retrofit, scenario 2. The simulated temperatures (lines) with different inner surface heat resistance R_{si} ($m^2\,K\,W^{-1}$) are compared with the measured values (points), considering measurement errors equal to $\pm 0.5\,^{\circ}C$.

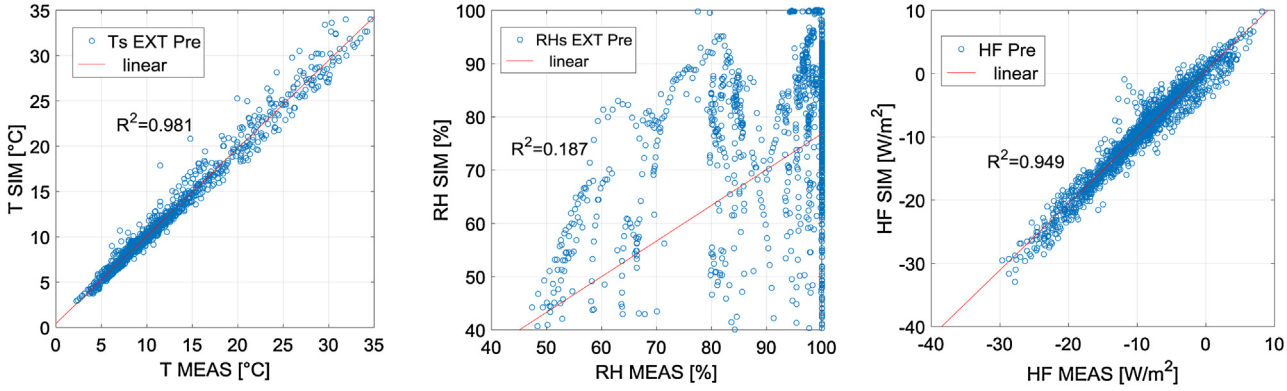

Fig. 7. Scattering graph and coefficient of determination R^2. Relation between measurements (x-axis) and calculation (y-axis). Comparison for T, RH and HF, heat flux, section B.1 East wall, before retrofit (Pre), Scenario2.

at lab scale. After that, they have been modified by their increasing/decreasing, evaluating also the plausibility (Table 6). As result, in terms of just moisture dependence of thermal conductivity, the effect is not prevalent with respect to other parameters.

In general, as expected, the temperature field is not significantly affected by the parameter changes.

For the heat flux the results differ. The worst case is for the kit A.2 with large gap between maximum and minimum and an overall underestimation of the heat flux. The best fit is represented

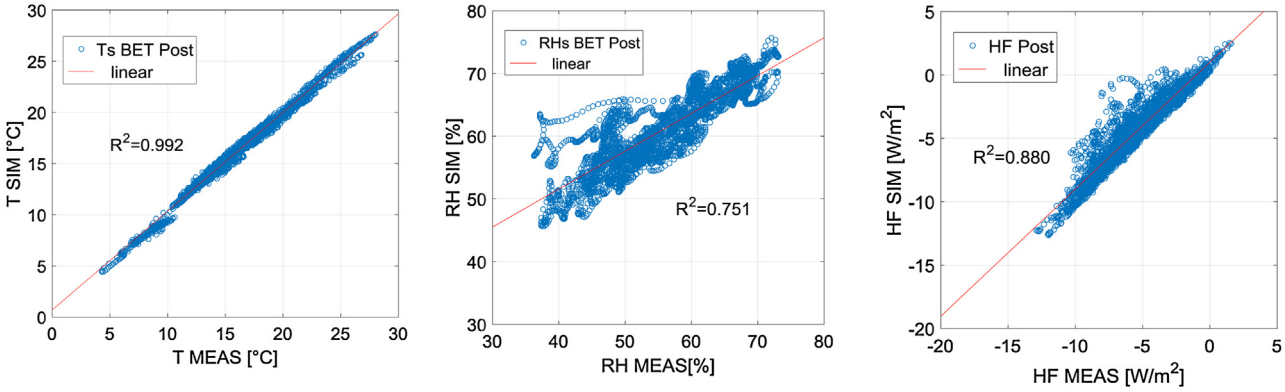

Fig. 8. Scattering graph and coefficient of determination R^2. Relation between measurements (x-axis) and calculation (y-axis). Comparison for T, RH at sensor position between base wall and insulation, and HF, heat flux, section B.1 East wall, after retrofit (Post), Scenario 3.

Table 6
Outline of the validation process, scenario 3 and scenario 4. (BET: at cold face of insulation, GAP: air cavity).

Retrofitted wall validation process	
Scenario 3	
Simulation vs monitoring	
HF_{SIM}	HF_{MEAS}
$T_{BET\ SIM}$	$T_{BET\ MEAS}$
$RH_{BET\ SIM}$	$RH_{BET\ MEAS}$
$T_{GAP\ SIM}$	$T_{GAP\ MEAS}$
$RH_{GAP\ SIM}$	$RH_{GAP\ MEAS}$
Parametric analysis	
Moisture-dep. thermal conductivity supplement (%/-M%):	
– aerogel mat: as measured (moist. dep λ) – 8.0	
– perlite mat: 1.8 – 4	
– loose perlite: 1.3 – 2.6	
s_d – value (thickness or μ):	
– cement based adhesive render μ: 9.8 – 98, thick: 1 – 3 – 4 – 5 mm	
– resin based adhesive render μ: 210 – 21, thick: 1– 3 – 4 – 5 mm	
Scenario 4	
Simulation vs monitoring	
HF_{SIM}	HF_{MEAS}
$T_{S\ SIM}$	$T_{S\ MEAS}$
$RH_{S\ SIM}$	$RH_{S\ MEAS}$
$T_{BET\ SIM}$	$T_{BET\ MEAS}$
$RH_{BET\ SIM}$	$RH_{BET\ MEAS}$
$T_{GAP\ SIM}$	$T_{GAP\ MEAS}$
$RH_{GAP\ SIM}$	$RH_{GAP\ MEAS}$
Parametric analysis	
s_d-value (m) of inner coating for A.1 and B.1:	
– resin finishing coat: 0 – 0.1 – 0.3 – 0.5- no render	
– tri-laminated PES fabric for B.2: 0 – 0.08 – 0.5	

by the kit B.2, where the median is almost zero, followed by the kit A.1 where the median is almost 1 $W\,m^{-2}$, shifted above zero. The same happens for B.1 but with higher variations in quartiles. It means that the heat flux is overestimated for A.1 and B.1 in the model with respect to the measurements, even if the simulated courses run generally within the ±8% error of the measured one. The overestimation for A.1 and B.1 is equivalent to have an insulation layer one-fourth less performing. For A.2 the underestimation, with RMSD almost 2 $W\,m^{-2}$, is explicable by high fluctuations above and below zero in the in-situ heat flux measurements. The reason could be some heating and cooling source near the sensors applied on the inner surface.

For the relative humidity, the gap between simulated and measured values is high, with an overestimation, with RMSD around 5% for the relative humidity measured at the interface between the insulation and the base wall, and around 8% for the relative humidity in the air gap.

In order to have acceptable results, by changing the μ-value of the render, the factor should be reduced of 10-times, for instance from 210 to 21. Because it is unrealistic, the last and more likely possibility is represented by changing the thickness of the layers. In fact, changing the initial thickness of 5 mm to 3 mm, the relative humidity is optimized (Table 7). This alternative is plausible due to the irregularity of thickness at installation site.

Within "Scenario 4" also the calculated outer and inner surface temperature and relative humidity are compared with the measured ones. Boxplots prove higher variability of the correlation in respect to "Scenario 3", especially for the relative humidity. The most sensitive are the external measurements both temperature and humidity (Fig. 9). This variability is due to two main points: the storage of water (relative humidity of 100%) by in-situ sensors after a rain event, due also to condensation under the protective aluminium tape, and the different irradiance during the day at different points of the wall.

For the first case, in the model, the relative humidity on the external surface is in equilibrium with the air relative humidity, and the low water absorption of tiles does not permit reaching the 100% RH over time, because at the end of a rain event the water quickly dries off. For the second case, the pyranometer, installed near the corner of the wall, has three different distances from the three temperature sensors installed in correspondence to each section of insulating retrofit kit at the East side. For that reason, the measured surface temperature, which depends on the irradiance, is shifted over time with respect to the measured irradiance.

For the internal surface and the interface between insulation and base wall, a distinct analysis is needed for the retrofit type B.2. Due to very low inner temperatures (about 10 °C) measured in December, when the heating system was switched off, the dew-

Table 7
Root mean square deviation of rel. humidity in case of different render thickness. The optimum value is achieved for 3 mm thickness of the render.

RMSD	RHs BET – render 1 mm	RHs BET – render 3 mm	RHs BET – render 4 mm	RHs BET – render 5 mm
PostB1	4.8822	4.5945	4.7311	7.008

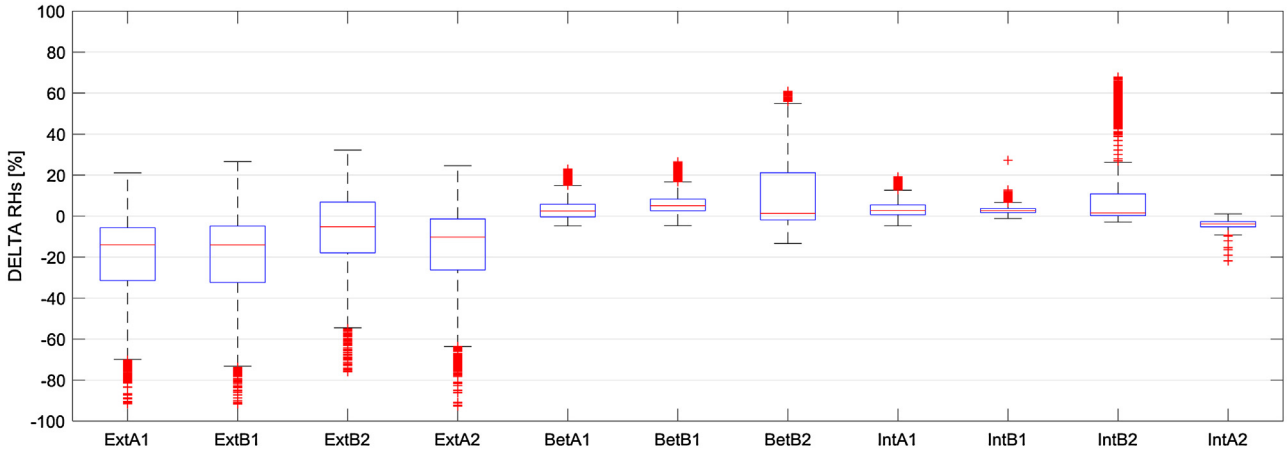

Fig. 9. Scenario 3, difference between simulated and measured relative humidity. Each boxplot refers to a different retrofit and a different sensor (Ext: external surface, Bet: between wall and insulation layer, Int: Internal surface).

point is reached at the interface inside the Wufi model. However, the condensation does not occur in the real site (Fig. 9).

For parametric analysis the s_d-value of the inner finishing (equal to 0.3 m for the resin-based coat, on the basis of lab measures) has been considered, in order to optimize the correspondence between simulation and measurement. The best fitting occurs when a lower value is used in calculation. It is true in light of the fact that in the reality the water vapour exchange to the inner side (moisture buffering) is higher with respect to the simulated one.

5.4. Transient U-value and performance analysis

In the light of the previous results and in order to predict the overall behaviour of the assemblies, the numerical calculation in Wufi® has been carried out considering also, as external climate, a whole Test Reference Year (TRY). The weather file created by IBP is based on measured data from the period 2000 to 2010 of ARPA Lombardia validated and completed by Politecnico di Milano.

In that way, the typical reference year of Milan has been used instead of the monitored data. The wall in the model is facing the same as in reality. The indoor climate is deducted from the exterior one and in conformity with the standard EN15026, with internal normal moisture load. All the data related to the assembly properties have been already discussed in the previous paragraphs.

The reason for this analysis is to have more reliable data about water content inside the layers, under the fact that can be verified if the equilibrium has been reached during a longer period. In addition, the un-retrofitted can be compared with the retrofitted wall using the same boundary conditions (in the previous analysis we had inevitably two consecutive periods as reference).

The effect of retrofits on the base wall has been evaluated. The changes of temperature and relative humidity, at the inter-face between insulation and masonry and at the inner surface as well, are not critical, in fact for neither of the kits value of 80% RH is reached. Consecutively, neither the water content in the inner plaster behind the insulation reaches high values. For that reason they are not shown here.

The transient U-value at the third year of simulation has been plotted in Fig. 10. Apart from the difference of the mean transmittance value, the trend over time is the same for each kit, with higher values in winter.

6. Discussion of the results

Besides determining the thermal transmittance of the wall, before and after retrofit, by means of average method, dynamic analysis method, and heat and moisture transfer model, the effect of the main involved parameters on the results has been investigated.

During the validation process, the error in measurements has always been taken into account. For an optimal correlation between measurements and calculation, it is adequate that the trends obtained from simulations fall on the range of the operational errors of the sensors. The correlation can be considered good if the trend is within the ±8% of the heat flux, within 0.5 °C for temperature and 5% for relative humidity.

In case of the outside surface the low correlation between measured and simulated relative humidity is due to the accumulation of moisture at the probes in-situ. The type of the sensors protection (aluminium tape) can in fact strongly affect the amount of relative humidity detected and the surface temperature as well. It should be taken into account during the simulation if the external surface temperature is used as input or as a point of comparison for validation as well.

Also other surface characteristics should be taken into account. In our case the optimal value of solar absorbance has been found as an average between tiles and the protective aluminium tape.

For the external surface it has been demonstrated that, in case of using, as input in the model, air temperature measured in proximity of the wall, no other data as wind-dependant resistance or long-emissivity exchange data are necessary, just the solar irradiance is needed. For those reason the constant surface heat resistance of 0.0588 $m^2\,K\,W^{-1}$ is found accurate for simulation, and more correct with respect to the value 0.04 $m^2\,K\,W^{-1}$, as demonstrated in the previous analysis.

For the internal surface the surface heat resistance plays a fundamental role for a good correlation. The convective air flow near to the wall, more or less intense, changes significantly the inner surface temperatures and consecutively the heat flux. For considering the right contribution of convective flow on the surface, a resistance

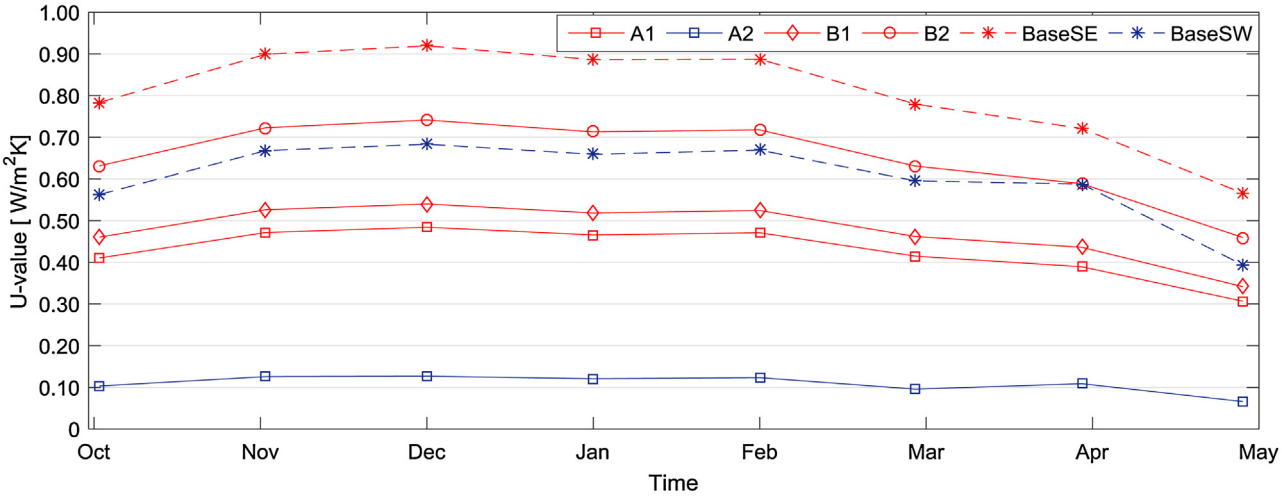

Fig. 10. Simulated transient U-value over 3rd year, all retrofit kits, compared to the base East and West wall.

Table 8
U-value of the wall after retrofit. Comparison among methods.

AFTER RETROFIT	U_{ST}	$U_{ST\ CORRECTED}$	U_{AM}	$U_{AM\ CORRECTED}$	U_{DYN}	$U_{DYN\ CORRECTED}$	$U_{SIM\ SCENARIO\ WUFI}$	$U_{SIM\ TRY\ WUFI}$
($W\,m^{-2}\,K^{-1}$)								
A.1	0.48	0.45	0.57	0.53	0.55	0.51	0.48	0.45
B.1	0.52	0.49	0.62	0.57	0.60	0.56	0.53	0.50
B.2	0.73	0.66	0.78	0.70	0.78	0.71	0.72	0.68
A.2	0.12	0.12	–	–	0.09	0.09	0.14	0.12

equal to 0.250 $m^2\,K\,W^{-1}$ should be used in our model. It depends on the low convective flow acting on that portion of the test wall. This value is also generally used in case of corners and at lower part of a wall.

The initial moisture content such as the boundary conditions are much influential. The initial moisture content within the assembly changes deeply the results if not more than one year of monitoring data is used and the equilibrium is not reached. The boundary condition effect is verified for both input data from measurement in-situ and input data from test reference year.

Thanks to the parametric analysis has been possible to evaluate that material parameters affect the results in different extent. As a demonstration of the state of the art regarding the heat and moisture transfer modelling, small changes of thermal conductivity do not affect the results sensitively: in our case, an increase or decrease of 25% of thermal conductivity is necessary to have enough substantial differences in the heat flux results.

The water vapour resistance of the adhesive and filler render does not affect the results by itself, (in our case 90% decreasing is needed to obtain countable differences in the results). However, changing the thickness of the render of few millimetres, the simulated relative humidity at the interface is optimized. This alternative agrees with the irregularity of thickness at installation site.

One point, not negligible, is related to the position of the sensors under the insulation board, so that the measurements feel the effect of the interface of the insulation layer. In fact, if the monitor position in the model is strictly close to the insulation, more conformity with the measurements can be read, with respect to a monitor position between base wall and adhesive render

From the results, a better fitting for kit A.1, B.1 and B.2. on the East wall with respect to A.2 on the West wall has been obtained. In case of A.2, most likely heating and cooling gains act on the inner surface.

The results in terms of the thermal transmittance obtained by the different methods are summarized and compared in Table 8.

For comparison reason, U_{ST}, U_{AM} and U_{DYN} have been also corrected using the same surface heat resistances optimized after the validation process in the Wufi model (R_{se} = 0.0588 $m^2\,K\,W^{-1}$, R_{si} = 0.250 $m^2\,K\,W^{-1}$).

In case of U_{SIM} (Wufi scenario, with monitored data as input), the difference with the other methods is satisfactory, being between 2% and 7%. When a reference weather file for Milan is used ($U_{SIM\ TRY}$), the U-values obtained by the model are lower than the previous ones. In that case the difference became of about 12% and it was a proof how much the different weather conditions, in the same climatic context, same period and same orientation, affect the results.

7. Conclusions

The main objective of this research consisted in assessing the transient hygrothermal behaviour of prototype insulating kits for the internal retrofitting of the wall.

The developed inner retrofit kits are: A.1, an improved and hydrophobized perlite board; B.1, a prefabricated multi-layer solution composed by three aerogel blankets, pre-coupled with a rigid finishing board; and B.2, a permeable wallpaper composed by one layer of aerogel blanket and finishing fabric. Besides them, also A.2, a loose-fill hydrophobized natural perlite for cavity wall has been investigated.

Those inner solutions have been designed to be lightweight and easy to apply, especially in the case of the aerogel wallpaper, which is handled by one and easy to fix on the wall. Each one of them has different thermal resistance, depending on the thickness and the thermal conductivity of the insulation materials. The perlite board has λ_{dry} equal to 0.063 $W\,m^{-1}\,K^{-1}$, the aerogel-polyester blanket has λ_{dry} equal to 0.025 $W\,m^{-1}\,K^{-1}$.

The part of research described here is summarized as follow:

– Within the parametric analysis, for the validation of the model with respect to the measures, the number of unknown variables is reduced at each following step of analysis.

- From the comparison a best fit for the temperature courses, admissible values for heat flux and some disagreement for relative humidity have been found.
- The material parameters play an important role in the modelling (especially in case of aerogel material), but slight variation does not affect the results of heat flux or temperature.
- Small changes of thermal conductivity do not affect the results sensitively.
- The water vapour resistance of the adhesive and filler render does not affect the results by itself, but the changed thickness of the render optimized the simulated relative humidity.
- Has been demonstrated that the boundary conditions, such as the surface heat resistance, are much more influential in respect to material parameters.
- The comparison between the methods for U-value calculation revealed the extent of percentage difference in the results.

The followed procedure represents a valid instrument for the evaluation of the behaviour, in case the reliability of the performance over time needs to be demonstrated for novel material appearing on the market.

In a further step of analysis, the long-term performance will be forecast, answering to the questions: how different climatic contexts and different type of masonry affect the results and which are the most critical condition for the performance decay, especially in case of low U-value.

Acknowledgments

The present investigation has got financial support from the EU FP7 2007/2013 under Grant Agreement n. EeB.NMP.2011-3–285540. The research EASEE project (Work Package 4 and Work Package 7), is the result of the collaboration of: Politecnico di Milano, National Technical University of Athens, Ridan Sp.zoo, Schwenk Putzetchnik GambH & Co. KG, D'Appolonia S.p.A., S&B Industrial Minerals, and Empa-Swiss Federal Laboratories for Materials Science and Technology. The technical support of R. Bischof (DECENTLAB) and R. Vonbank (Empa) is highly appreciated.

References

[1] Directive 2012/27/EU, online at http://www.buildup.eu/publications/32236.
[2] (WBCSD) Energy Efficiency in Buildings—Transforming the Market, World Business Council for Sustainable Development, Geneva, 2009.
[3] J. Kosny, A. Fallahi, N. Shukla, Cold Climate Building Enclosure Solutions, National Renewable Energy Laboratory (NREL), Golden, CO, 2013 (No. DOE/GO-102013-3718).
[4] R. Baetens, B.P. Jelle, A. Gustavsen, Aerogel insulation for building applications: a state-of-the-art review, Energy Build. 43 (4) (2011) 761–769.
[5] M. Koebel, A. Rigacci, P. Achard, Aerogel-based thermal superinsulation: an overview, J. Sol-Gel Sci. Technol. 63 (3) (2012) 315–339.
[6] E. Cuce, P.M. Cuce, C.J. Wood, S.B. Riffat, Toward aerogel based thermal superinsulation in buildings: a comprehensive review, Renew. Sustainable Energy Rev. 34 (2014) 273–299.
[7] T. Stahl, S. Brunner, M. Zimmermann, K. Ghazi Wakili, Thermo-hygric properties of a newly developed aerogel based insulation rendering for both exterior and interior applications, Energy Build. 44 (2012) 114–117.
[8] M.A. Aegerter, N. Leventis, M.M. Koebel, Aerogels Handbook, Springer Science & Business Media, 2011.
[9] A.S. Dorcheh, M.H. Abbasi, Silica aerogel: synthesis properties and characterization, J. Mater. Process. Technol. 199 (1) (2008) 10–26.
[10] S. Pallin, A.S. Kalagasidis, Hygrothermal Risk Assessment-Retrofit of External Wall by the Application of Interior Insulation (2014).
[11] J. Straube, C. Schumacher, Assessing the Durability Impacts of Energy Efficient Enclosure Upgrades using Hygrothermal Modeling (2006).
[12] J. Straube, K. Ueno, C. Schumacher, Internal Insulation of Masonry Walls: Final Measure Guideline, Prepared for US Department of Energy, Office of Energy Efficiency and Renewable Energy, 2011.
[13] A. Holm, H. M. Kuenzel, Uncertainty Approaches for hygrothermal building simulations-drying of an AAC flat roof in different climates, IPS Conference Building Simulation (2001, August).
[14] H.S. Hens, Heat, Air and Moisture Transfer in Highly Insulated Building Envelopes (Hamtie), FaberMaunsell Limited, 2002.
[15] M. Guizzardi, D. Derome, R. Vonbank, J. Carmeliet, Hygrothermal behavior of a massive wall with interior insulation during wetting, Build. Environ. 89 (2015) 59–71.
[16] Y. Zhang, K. Du, J. He, L. Yang, Y. Li, S. Li, Impact factors analysis on the thermal performance of hollow block wall, Energy Build. 75 (2014) 330–341.
[17] E. Vereecken, L. Van Gelder, H. Janssen, S. Roels, Interior insulation for wall retrofitting–a probabilistic analysis of energy savings and hygrothermal risks, Energy Build. 89 (2015) 231–244.
[18] J. Zhao, R. Plagge, J. Grunewald, Performance assessment of interior insulations by stochastic method, 9th Nordic Symposium on Building Physics–NSB, (2011, June).
[19] H.S.L.C. Hens, Modeling the heat air, and moisture response of building envelopes: what material properties are needed, how truthful are the predictions? J. ASTM Int. 4 (2) (2007) 1–11.
[20] P. Johansson, S. Geving, C.E. Hagentoft, B.P. Jelle, E. Rognvik, A.S. Kalagasidis, B. Time, Interior insulation retrofit of a historical brick wall using vacuum insulation panels: hygrothermal numerical simulations and laboratory investigations, Build. Environ. 79 (2014) 31–45.
[21] K. Ghazi Wakili, B. Binder, M. Zimmermann, C. Tanner, Efficiency verification of a combination of high performance and conventional insulation layers in retrofitting a 130-year old building, Energy Build. 82 (2014) 237–242.
[22] P.A. Moradias, P.D. Silva, J.P. Castro-Gomes, M.V. Salazar, L. Pires, Experimental study on hygrothermal behaviour of retrofit solutions applied to old building walls, Constr. Build. Mater. 35 (2012) 864–873.
[23] F. Ascione, F. De Rossi, G.P. Vanoli, Energy retrofit of historical buildings: theoretical and experimental investigations for the modelling of reliable performance scenarios, Energy Build. 43 (8) (2011) 1925–1936.
[24] P.G. Cesaratto, M. De Carli, S. Marinetti, Effect of different parameters on the in situ thermal conductance evaluation, Energy Build. 43 (7) (2011) 1792–1801.
[25] J. Toman, A. Vimmrova, R.Černý, Long-term on-site assessment of hygrothermal performance of interior thermal insulation system without water vapour barrier, Energy Build. 41 (1) (2009) 51–55.
[26] Z. Pavlík, R.Černý, Experimental assessment of hygrothermal performance of an interior thermal insulation system using a laboratory technique simulating on-site conditions, Energy Build. 40 (5) (2008) 673–678.
[27] Z. Pavlík, R.Černý, Hygrothermal performance study of an innovative interior thermal insulation system, Appl. Therm. Eng. 29 (10) (2009) 1941–1946.
[28] M. Cucumo, A. De Rosa, V. Ferraro, D. Kaliakatsos, V. Marinelli, A method for the experimental evaluation in situ of the wall conductance, Energy Build. 38 (3) (2006) 238–244.
[29] S. Brunner, H. Simmler, In situ performance assessment of vacuum insulation panels in a flat roof construction, Vacuum 82 (7) (2008) 700–707.
[30] J. Straube, C. Schumacher, Interior insulation retrofits of load-bearing masonry walls in cold climates, Build. Sci. Dig. 114 (2007) 1–16.
[31] T. Nussbaumer, K. Ghazi Wakili, C. Tanner, Experimental and numerical investigation of the thermal performance of a protected vacuum-insulation system applied to a concrete wall, Appl. Energy 83 (8) (2006) 841–855.
[32] EASEE—Envelope Approach to improve Sustainability and Energy Efficiency in existing multi-storey multi owner residential building Project. Online at www.easee-project.eu/home.
[33] EN 1745. 2012 Masonry and masonry products—methods for determining thermal properties.
[34] EN ISO 6946. 2008 Building components and building elements. Thermal resistance and thermal transmittance. Calculation method.
[35] J.C. Wong, H. Kaymak, S. Brunner, M.M. Koebel, Mechanical properties of monolithic silica aerogels made from polyethoxydisiloxanes, Microporous Mesoporous Mater. 183 (2014) 23–29.
[36] ISO 9869-1:2014 Thermal insulation – Building elements – In-situ measurement of thermal resistance and thermal transmittance – Part 1: Heat flow meter method.
[37] H.M. Künzel, Simultaneous Heat and Moisture Transport in Building Components One-and Two-dimensional Calculation Using Simple Parameters, IRB, Verlag Stuttgart, 1995.
[38] EN 15026. 2008. Hygrothermal performance of building components and building elements. Assessment of moisture transfer by numerical simulation.
[39] ISO 10456:2007. Building materials and products – Hygrothermal properties – Tabulated design values and procedures for determining declared and design thermal values.
[40] P.W. Steskens, H. Janssen, C. Rode, Influence of the convective surface transfer coefficients on the Heat Air, and Moisture (HAM) building performance, Indoor Built Environ. 18 (3) (2009) 245–256.
[41] H.J. Steeman, A. Janssens, M. De Paepe, On the applicability of the heat and mass transfer analogy in indoor air flows, Int. J. Heat Mass Transfer 52 (5) (2009) 1431–1442.
[42] I. Beausoleil-Morrison, The adaptive simulation of convective heat transfer at internal building surfaces, Build. Environ. 37 (8) (2002) 791–798.